MIMO Spatial Turbo Coding with Iterative Equalization

Khoirul Anwar* and Tadashi Matsumoto*,‡
*Japan Advanced Institute of Science and Technology (JAIST), 1-1 Asahidai, Nomi, Ishikawa, 923-1292 Japan
E-mail:{anwar-k, matumoto}@jaist.ac.jp
‡Center for Wireless Communications, University of Oulu, FI-90014 Finland
E-mail: tadashi.matsumoto@ee.oulu.fi

***Abstract*—This paper proposes a structure that combines iterative equalization and turbo decoding, denoted as spatial turbo coding (STC), for single carrier signaling to achieve near capacity performance in multipath-rich fading channels. Instead of multiplexing the encoded bits in the time domain as in the standard turbo codes, the proposed STC transmits coded bits in the space domain by employing multiple-input multiple-output (MIMO) transceiver to exploit space diversity, path diversity and coding gains through the decoding branches at the receiver. The considered MIMO detector is a MIMO frequency domain soft-cancelation and minimum mean square error equalizer (FD/SC-MMSE). Extrinsic Information Transfer (EXIT) chart analysis confirms that bit-error-rate (BER) pinch-off is achieved in 64-path Rayleigh fading channels with equal average path gains power which is just by about 1dB away from the static channel capacity/dimension of 2×2 MIMO systems.**

***Index Terms*—MIMO; Turbo equalization; EXIT.**

I. Introduction

An application of the Turbo principle is Space-Time Turbo Code such as in [1], [2] and more references there in. The design criterion should be in such a way to achieve maximum spatial diversity and coding gain, assuming flat fading. Furthermore, as the knowledge of the authors, the [3] is the only publication that aims to combine the spatial diversity, path diversity, and turbo coding gain in frequency selective channels.

However, [3] does not examine suitable constituent encoders in detail which is required in the design of iterative detection. Furthermore, there is no explanation about the fact that the "vertical iteration" (of which definition is provided later) can be seen as a decoding process of the parallel concatenated turbo code itself.

This paper is aiming to provide in depth contributions on the technique in [3] by providing more thorough investigations on constituent encoder and convergence properties. The proposed structure is very simple: multiple transmit antennas are connected to the same information source, and each antenna has its own encoder, separated by an interleaver from the other antennas; This structure is referred to as *spatial turbo coding*. At the receiver side, two iterative processes are invoked, one is *horizontal iteration (HI)* and the other *vertical iteration (VI)*.

The *HI* performs turbo equalization with the aim of combining all the multi-path channel energies and achieving path diversity gain, while eliminating the inter-antenna interference (IAI) components from other antennas. *VI* is used to further enhance the performance, aiming at achieving coding gain on the top of the diversity gain. In fact, *VI* loop is exactly the same as the turbo loop in the parallel concatenated turbo decoder. The only difference from the standard turbo code is, as a whole, that in the standard parallel concatenated codes, the encoded sequence is multiplexed in the time domain, while the spatial turbo code case, the multiplexing is in the spatial domain with aims of combining the turbo equalization and turbo decoding at the receiver side.

The latest version of turbo equalization, frequency domain soft cancellation and minimum mean squared error (FD/SC-MMSE) [4], is used in this paper because so far as the authors' knowledge, it is most efficient equalization technique in terms of performance and complexity. However, it should be noted here that the general concept of STC is independent of the equalizer type, e.g., maximum *a* posteriori probability (MAP) equalizer can achieve obviously better performance than FD/SC-MMSE, which is a matter of the complexity-performance trade-off.

This paper is organized as follows. We start by presenting the system model in Section II. The proposed STC design is discussed in Section III, which is followed by investigation on the selection of the constituent encoders and their analysis in Section IV using extrinsic information transfer (EXIT) chart. Section V presents the performance evaluation in terms of bit-error rate (BER). Finally, conclusion is given in Section V.

In the following, vectors are marked with bold lowercase and matrices with bold uppercase notations. An operator $diag(\cdot)$ with a vector argument denotes a diagonal matrix with vector elements on its diagonal components. An estimate of variable is denoted by $\hat{(\cdot)}$. Operator $(\cdot)^H$ denotes a hermitian for a complex conjugation. An identity matrix is denoted as $\mathbf{I}$, while the matrix transpose operator is denoted as $(\cdot)^T$.

II. System Model

In the transmitter, there are two sources of information bits, b_1 and b_2, as shown in Fig. 1. The bit stream of the first source, b_1, is encoded by the encoder C_1, interleaved by Π_1 and transmitted from antenna branch #1. Similarly to b_1, bit stream b_2 is encoded by encoder C_2, interleaved by Π_2 and sent from antenna branch #2. Puncturing may be performed to adjust the code rate. Multiplexing the output of the encoders such as in

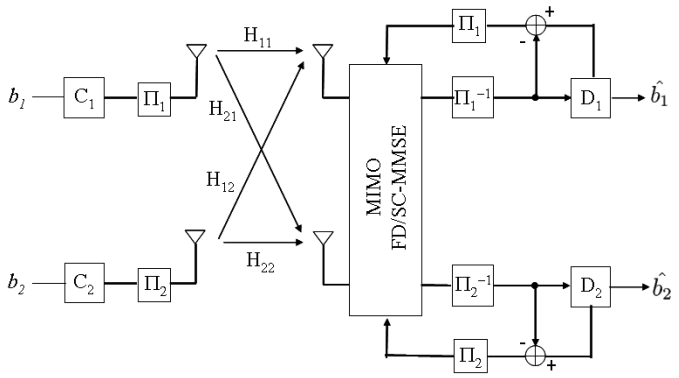

Fig. 1. Typical Structure of (Two-user) MIMO with Turbo Equalization

[5] is not applied, because it causes performance degradation especially when the code rate is high [6]. We consider single carrier (SC) signaling system. The encoded symbols from the two transmitters are transmitted simultaneously over the MIMO frequency selective fading channel.

Frequency domain processing is considered because of its low computational complexity. All symbols are represented and performed in block wise format. The encoded information bits by a channel code in each antenna branch are interleaved, segmented and BPSK mapped length K symbol block. Then, symbol block vector to be transmitted from the m-th transmit antenna is expressed as

$$\mathbf{s}_m = [s_m(1), s_m(2), \ldots, s_m(K)]^T, \tag{1}$$

Then, the symbol block vector over all transmit antennas is given by

$$\mathbf{s} = [\mathbf{s}_1, \mathbf{s}_2, \ldots, \mathbf{s}_M)]^T. \tag{2}$$

The channel is assumed to be static within a block (block-fading Rayleigh fading channel), where the fading coefficients are assumed to change in an independent and identically distributed (i.i.d.) manner block-by-block as well as between the antennas (there is no spatial correlation between antenna). The space-time L multipath propagation channel matrix $\mathbf{H}$ is given by

$$\mathbf{H} = \begin{bmatrix} \mathbf{H}_{11} & \mathbf{H}_{12} & \ldots & \mathbf{H}_{1M} \\ \mathbf{H}_{21} & \mathbf{H}_{22} & \ldots & \mathbf{H}_{2M} \\ \vdots & \vdots & \ddots & \vdots \\ \mathbf{H}_{N1} & \mathbf{H}_{N2} & \ldots & \mathbf{H}_{NM} \end{bmatrix}, \tag{3}$$

where each submatrix $\mathbf{H}_{nm}$, $n = 1, 2, \cdots, N$, $m = 1, 2, \cdots, M$, is a toeplitz matrix. M and N is numbers of transmit and receive antennas, respectively.

With the cyclic prefix (CP) transmission, each submatrix $\mathbf{H}_{nm}$ becomes circulant with multipath channel response on its first column,

$$\mathbf{h}_{nm} = [h_{nm}(0), h_{nm}(1), \cdots, h_{nm}(L-1), 0, \cdots, 0,]^T, \tag{4}$$

where $L-1$ is channel memory length, $h_{nm}(\ell)$ the impulse response between m-th Tx and n-th Rx antennas, and the whole matrix $\mathbf{H}$ given by (3) becomes a circulant-block matrix.

Now we can utilize the characteristic of the circularity of matrix $\mathbf{H}$ to obtain equivalent frequency domain channel matrix

$$\begin{aligned} \mathbf{\Xi} &= \mathbf{F}_N^H \mathbf{H} \mathbf{F}_M \\ &= \begin{bmatrix} \mathbf{\Xi}_{1,1} & \mathbf{\Xi}_{1,2} & \cdots & \mathbf{\Xi}_{1,M} \\ \mathbf{\Xi}_{2,1} & \mathbf{\Xi}_{2,2} & \cdots & \mathbf{\Xi}_{2,M} \\ \vdots & \vdots & \ddots & \vdots \\ \mathbf{\Xi}_{N,1} & \mathbf{\Xi}_{N,2} & \cdots & \mathbf{\Xi}_{N,M} \end{bmatrix}, \end{aligned} \tag{5}$$

with $\mathbf{F}_N = \mathbf{I}_N \otimes \mathbf{F}$, $\mathbf{I}_N$ is an identity matrix of dimension N, $\otimes$ denotes the Kronecker product and $\mathbf{F}$ is discrete Fourier matrix, of which element given by

$$\mathbf{F}_{i,j} = \frac{1}{\sqrt{K}} e^{\jmath \cdot \frac{2\pi}{K} \cdot i \cdot j}, \tag{6}$$

where $\jmath = \sqrt{-1}$ and $i, j = 0, \cdots, K-1$.

We denote the m-th column submatrix in (3) and (5) as $\mathbf{H}_m$ and $\mathbf{\Xi}_m$, respectively. The component of $\mathbf{\Xi}$ for the m-th transmit antenna, $\mathbf{\Xi}_m$, can also be obtained from its time-domain representation by

$$\mathbf{\Xi}_m = \mathbf{F}_N^H \mathbf{H}_m \mathbf{F}_M. \tag{7}$$

When the block of symbol in (2) is transmitted over the frequency selective fading channel, the received signal can be expressed as

$$\mathbf{r} = \mathbf{H}\mathbf{s} + \nu, \tag{8}$$

where ν is a zero mean complex additive white Gaussian noise vector with covariance $\mathbf{E}\{\nu\nu^H\} = \sigma^2\mathbf{I}$. σ^2 denotes the noise variance defined by the specified signal to noise ratio (SNR) per antenna branch in decibel (dB), as

$$\sigma^2 = 10^{-\mathbf{SNR}[\mathrm{dB}]/10}. \tag{9}$$

III. The Proposed Spatial Turbo Coding

MIMO system with 2×2 transmit (Tx) and receive (Rx) antennas is assumed in this paper, but its extension to a more generic MIMO structure is rather straightforward.

A. Transceiver Structure

As shown by Fig. 1, sources b_1 and b_2 are uncorrelated. We propose an STC structure by assuming that bitstream b_2 is Π_0 spatially interleaved version of b_1 as described by Fig. 2. Therefore, $d = b_2$ and $b = b_1$. There are three interleavers and two encoders at the transmitter. At the receiver, turbo equalizer is utilized.

In detail, the STC comprises of turbo equalizer that utilizes soft input LLR and provides soft output LLR, Bahl-Cocke-Jelinek-Raviv (BCJR) [7] decoders and three interleavers Π_1, Π_2 to interleave the extrinsic LLR of the coded bits and Π_0 to interleave the extrinsic LLR of uncoded bits whose length is shorter than the previous two interleavers.

The receiver consists of the common MIMO FD/SC-MMSE equalizer, which is performed in the frequency domain, and 2

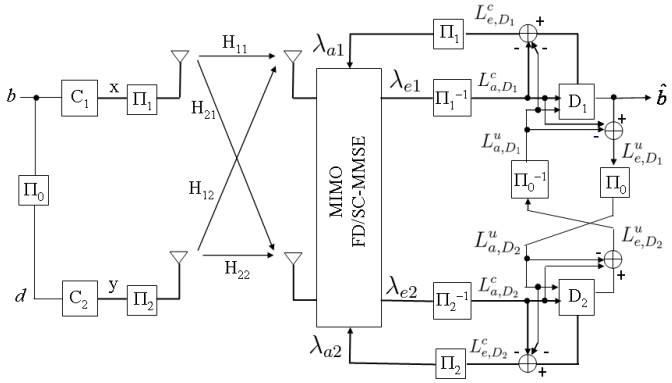

Fig. 2. The proposed STC: Encoders C_1 and C_1 are SRCC codes

decoder branches D_1 and D_2. We consider the Bahl-Cocke-Jelinek-Raviv (BCJR) algorithm [7] as the MAP decoder of the codes.

The novelty of this structure is that beside the coding gain obtained by performing turbo (vertical) iteration between decoders D_1 and D_2, the additional coding gain can be obtained by turbo (horizontal) iteration between equalizer and decoders D_1 and D_2. However, the gain of traditional turbo code is obtained only by the turbo (vertical) iteration between the D_1 and D_2.

The iteration is performed between FD/SC-MMSE and the decoders according to the standard turbo principle. The FD/SC-MMSE iteration for equalization takes place independently in each horizontal loop via the connection between FD/SC-MMSE equalizer and each corresponding decoder.

After the first *HI*, the FD/SC-MMSE delivers extrinsic information in the form of log-likelihood ratio (LLR) of the coded bits to the each decoder. After the deinterleaving Π_1^{-1} and Π_2^{-1}, corresponding to the horizontal loops shown in upper and lower part of Fig. 1, respectively, the BCJR algorithm updates the extrinsic LLR which is fed back to the FD/SC-MMSE equalizer via the interleaver Π_1 and Π_2. The LLR is then used for interference cancelation in the next *HI*.

The other *VI* is performed between the decoder D_1 and D_2 via the spatial interleaver Π_0 and deinterleaver Π_0^{-1}. Compared to the HI, the VI transfers extrinsic information of the uncoded information bits. In order to activate the VI, the BCJR decoder D_1 and D_2 should be designed to adopt the extrinsic LLR of the uncoded information bits. The *VI*s provide additional coding gain on the top of the diversity gain achieved by the *HI*s.

B. Turbo Equalization

Because the FD/SC-MMSE and its extension into MIMO have been derived in detail by many publications, in this paper, we do not describe FD/SC-MMSE algorithm. Please see, for example, [8] and recent analytical method in [4] for more details.

In the first *HI*, the equalizer input *a* priori LLRs have initial value $\lambda_{a1} = \lambda_{a2} = 0$, which are then gradually increased in the next *HI* by the help of the decoders. The FD/SC-MMSE then gives outputs in the form of extrinsic LLR λ_{e1} and λ_{e2} for antenna 1 and 2, respectively. *A* priori LLR λ_a is then parameterized using the mutual information (MI) [9] between λ_a and transmitted symbol $\mathbf{s}$ (timing index is omitted for the simplicity), which is referred as horizontal *a* priori mutual information $\mathbf{I}_{a,E}$ (for antenna branch #1), defined as

$$\begin{aligned}\mathbf{I}_{a1,E} &= I(\lambda_{a1};\mathbf{x}) \\ &= \frac{1}{2}\cdot\sum_{s=-1,+1}\int_{-\infty}^{+\infty} p_a(\lambda_{a1}|s) \\ &\quad\cdot\log_2\frac{2\cdot p_a(\lambda_{a1}|s)}{p_a(\lambda_{a1}|s=+1)+p_a(\lambda_{a1}|s=-1)}d\lambda_{a1}, \end{aligned} \quad (10)$$

where p_a is the conditional probability density function of λ_{a1} given $s = \{-1, +1\}$. $\mathbf{I}_{a2,E}$ is also obtained in the same way as

$$\mathbf{I}_{a2,E} = I(\lambda_{a2};\mathbf{y}). \quad (11)$$

By following (10), MI of the extrinsic LLR, as the output of turbo equalizer can also be obtained as

$$\mathbf{I}_{e1,E} = I(\lambda_{e1};\mathbf{x}), \quad (12)$$
$$\mathbf{I}_{e2,E} = I(\lambda_{e2};\mathbf{y}). \quad (13)$$

Because the equalizer is connected to the channel, $I_{e,E}$ can be viewed as a function of both $I_{a,E}$ and the SNR. Therefore, the extrinsic information transfer characteristic $\mathbf{I}_{e,E}$ can be defined as

$$\mathbf{I}_{e1,E} = T_E(\mathbf{I}_{a1,E}, \mathbf{I}_{a2,E}, \mathrm{SNR}_1, \mathrm{SNR}_2), \quad (14)$$
$$\mathbf{I}_{e2,E} = T_E(\mathbf{I}_{a2,E}, \mathbf{I}_{a2,E}, \mathrm{SNR}_1, \mathrm{SNR}_2), \quad (15)$$

where T_E is a transfer function of the FD/SC-MMSE turbo equalizer, SNR_1 and SNR_2 is the SNR at antenna branch #1 and #2. In the following, we assume the condition

$$\mathrm{SNR}_1 = \mathrm{SNR}_2 \quad (16)$$

is always satisfied. Therefore, we can omit subscripts 1 and 2 for simple presentation.

IV. EXIT Analysis

We describe an analysis tool called extrinsic information transfer (EXIT) chart to evaluate the performance and observe the convergence of the proposed spatial turbo coding scheme.

A. The Constituent Encoders

In many references on space time turbo code such as [3], [10], [11] and [1], [5], the considered component decoders are nonsystematic nonrecursive convolutional codes (NSNRCC). Unfortunately, the NSNRCC is unsuitable for iterative decoding with the aim of minimizing the probability of error [12].

Each decoders in STC provides two output extrinsic LLRs, one output for *HI* iterations and the other for *VI* iterations. This fact shows that encoders/decoders should be designed very carefully, for example it should be NSNRCC or SRCC codes, to achieve as large performance gain as possible. With

the help by EXIT chart [9], it is easy to design a suitable codes for the STC structure.

After deinterleavers Π_1^{-1} and Π_2^{-1} are performed, the extrinsic LLR λ_{e1} and λ_{e2} from turbo equalizer are then used by the decoders D_1 and D_2 as the *a* priori LLR $\mathbf{L}^c_{a,D1}$ and $\mathbf{L}^c_{a,D2}$. Each decoder provides two output extrinsic LLRs, $\mathbf{L}^c_{e,D}$ for horizontal loop and $\mathbf{L}^u_{e,D}$ for vertical loop. $\mathbf{L}^c_e$ is the extrinsic LLR for the *coded information bits* which is required by the turbo equalizer and expressed in terms of mutual information as

$$\mathbf{I}^c_{a,D1} = I(L^c_{a,D1};\mathbf{x}), \quad \mathbf{I}^c_{e,D1} = I(L^c_{e,D1};\mathbf{x}), \tag{17}$$
$$\mathbf{I}^c_{a,D2} = I(L^c_{a,D2};\mathbf{y}), \quad \mathbf{I}^c_{e,D2} = I(L^c_{e,D2};\mathbf{y}), \tag{18}$$

while $\mathbf{L}^u_e$ is the extrinsic LLR of the *uncoded information bits* which is exchanged between the two decoders as

$$\mathbf{I}^u_{a,D1} = I(L^u_{a,D1};\mathbf{b}), \quad \mathbf{I}^u_{e,D1} = I(L^u_{e,D1};\mathbf{b}), \tag{19}$$
$$\mathbf{I}^u_{a,D2} = I(L^u_{a,D2};\mathbf{d}), \quad \mathbf{I}^u_{e,D1} = I(L^u_{e,D2};\mathbf{d}), \tag{20}$$

where $\mathbf{d}$ is the interleaved version of the uncoded bits $\mathbf{b}$.

By viewing the decoder as a transfer function T_D, the mutual information of extrinsic LLR of the coded information bits for decoder D_1 and D_2 are

$$I^c_{e,D1} = T_{D1}(I^c_{a,D1}, I^u_{a,D1}), \tag{21}$$
$$I^c_{e,D2} = T_{D2}(I^c_{a,D2}, I^u_{a,D2}), \tag{22}$$

and for uncoded information bits, it is

$$I^u_{e,D1} = T_{D1}(I^c_{a,D1}, I^u_{a,D1}), \tag{23}$$
$$I^u_{e,D2} = T_{D2}(I^c_{a,D2}, I^u_{a,D2}), \tag{24}$$

where $I^c_{a,D}$ and $I^u_{a,D}$ denote the mutual information for *a* priori LLRs of the coded and uncoded information bits provided by the equalizer (horizontal loop) and the other decoder (vertical loop), respectively. It indicates that output of decoders depend on the two components i.e. $I^c_{a,D}$ and $I^u_{a,D}$, which mean that the EXIT chart is three dimensional.

In this paper, we first evaluate NSNRCC and systematic recursive convolutional codes (SRCC) with memory length of 3 and octal notation of the code generator $(17, 15)$ as in [8]. The interleaver length Π_1 and Π_1 is 1024 and Π_0 is 512, which is long enough to perform *HI* and *VI* iterations in multipath-rich environment such as $L = 64$. Then, the convergence properties of the decoders for the NSNRCC and SRCC component encoders are observed for several $I^c_{a,D}$ and $I^u_{a,D}$ values ($\in [0, 1]$) to obtain their convergence behavior.

Fig. 3 shows the EXIT curves of NSNRCC and SRCC decoder at receive per-antenna SNR of -3.5dB. The EXIT curve is plotted when $I^u_{a,D_1} = I^u_{a,D_2}$. The curves of NSNRCC encoders cross each other before they reach the point (1,1). However, the curves with SRCC reach the point (1,1) without getting stuck at some points before the final point. Observing deeply on the SRCC decoder, we can expect a BER pinch-off.

Finally, we can conclude that STC should be accompanied by an SRCC component encoder to achieve a turbo cliff since the tunnel open suddenly to reach point (1,1). On the other hand, when NSNRCC is considered, the BER of STC is improved gradually without any turbo cliffs or pinch-off.

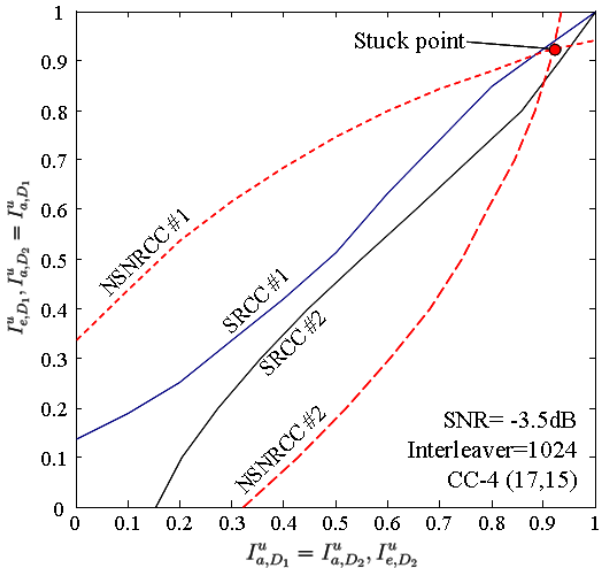

Fig. 3. EXIT Analysis on NSNRCC and SRCC Component Encoder

As a consequence of using SRCC, the uncoded LLR $\mathbf{L}^u_{e,D}$ for the *VI* is given by

$$\begin{aligned}\mathbf{L}^u_{e,D1} &= \mathbf{L}^u_{p,D1} - \mathbf{L}^u_{a,D1} - \mathbf{L}^c_{a,D1}\\ \mathbf{L}^u_{e,D2} &= \mathbf{L}^u_{p,D2} - \mathbf{L}^u_{a,D2} - \mathbf{L}^c_{a,D2},\end{aligned} \tag{25}$$

where $\mathbf{L}^u_{p,D}$ and $\mathbf{L}^{c'}_{a,D}$ are the *a* posteriori LLR of the uncoded bits at the output of BCJR and *a* priori LLR of the uncoded information bits received from the equalizer.

Similarly, the coded LLR $\mathbf{L}^c_{e,D}$ is

$$\begin{aligned}\mathbf{L}^c_{e,D1} &= \mathbf{L}^c_{p,D1} - \mathbf{L}^c_{a,D1} - \mathbf{L}^u_{a,D1}\\ \mathbf{L}^c_{e,D2} &= \mathbf{L}^c_{p,D2} - \mathbf{L}^c_{a,D2} - \mathbf{L}^u_{a,D2}.\end{aligned} \tag{26}$$

The receiver part of Fig. 2 shows the graphical representation of the (25) and (26).

The final output is taken from the *a* posteriori LLR of the uncoded information bits, $\mathbf{L}^u_{p,D1}$, from decoder D_1 as shown in Fig. 2. Obviously, it is also possible to obtain the final output from the *a* posteriori LLR $\mathbf{L}^u_{p,D2}$ after performing deinterleaving Π_0^{-1}.

B. 3D EXIT Chart

Equalizer has two input *a* priori LLRs, $L_{a1,E}$ and $L_{a2,E}$ and two output extrinsic LLRs, $L_{e1,E}$ and $L_{e2,E}$ for D_1 and D_2, respectively. Each decoder has two inputs, $L^u_{a,D}$ and $L^c_{a,D}$, and two outputs, $L^u_{e,D}$ and $L^c_{e,D}$ for uncoded and coded bits, respectively. The uncoded bits LLR is utilized for *VI*, while the coded bits LLR is for *HI*.

By assuming a fixed SNR_1 and SNR_2, the EXIT chart will be, therefore, in three dimension (3D) because of the two input LLRs which is from decoder D_1 and D_2. The observed 3D EXIT for the decoders is shown in Fig. 4 for decoder D_1.

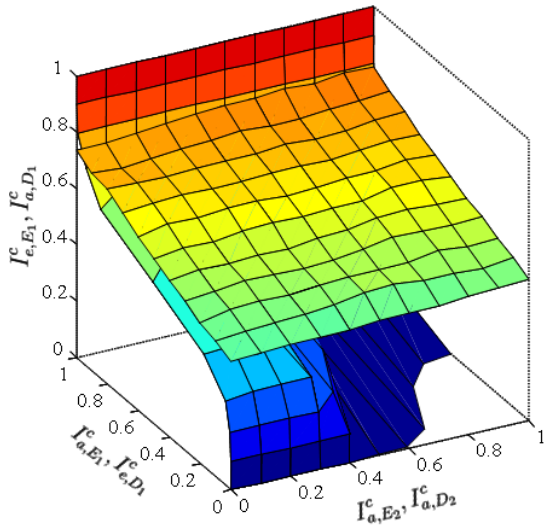

Fig. 4. 3D EXIT Analysis on STC

EXIT surface of the equalizer is plotted by assuming that per-antenna SNR is -3.5dB for a certain fixed $L = 64$ channel realization. For the *VI*, the decoders are not connected to the channel. Therefore, the decoder EXIT function is independent of the channel per-antenna SNR. Assuming an extreme condition when $I_{a,D1}$ is increasing eventhough $I_{a,D2} = 0$, the tunnel between MIMO-FD/SC-MMSE equalizer and two decoders still open as the SNR increases. Similarly, when $I_{a,D2} = 1$, the tunnel will suddenly open at lower SNR. As a consequence, the turbo cliff will happen.

In the turbo equalization-based receiver, equalization and decoding steps are iterated by passing LLR λ_e and $L^c_{e,D}$ between the receiver components. Here, we omit the subscripts 1 and 2. The iterative process starts with an initial equalization, where $\lambda_a = 0$, and therefore $I_{a,E} = 0$. Next, the output LLRs λ_e with $I_{e,E} = I^c_{a,D}$ are fed into the decoder yielding LLRs $L^c_{e,D}$ with $I^c_{e,D} = I_{a,E}$, which are fed back to the equalizer and so forth. This procedure is described in single EXIT chart combining equalizer and decoder, referred to as trajectory.

To analyze the trajectory of the iteration behavior, we use activation ordering with pattern of α(HβVγ). α expresses number of repetitions. γ is activation number of *HI*s and β denotes the activation number of *VI*s. The analysis on *HI* and *VI* in the form of trajectory is shown in Fig. 5 for per-antenna SNR = -3.5dB with pattern of 3(H1V5).

Fig. 5(a) shows that the *VI* converts curve of two SRCCs in to a curve of turbo code within 5 iterations. We also observe trajectory plots are well matched to the predicted the EXIT curves. The EXIT chart and trajectory of the *VI* are shown by Fig. 5(b) where 5 iterations were invoked in each trajectory.

It is found that the trajectories fall between the EXIT curves, with small gaps between them. This is due to the fact that the iteration number is fixed to 5 for each iteration, while the EXIT curves are drawn independently.

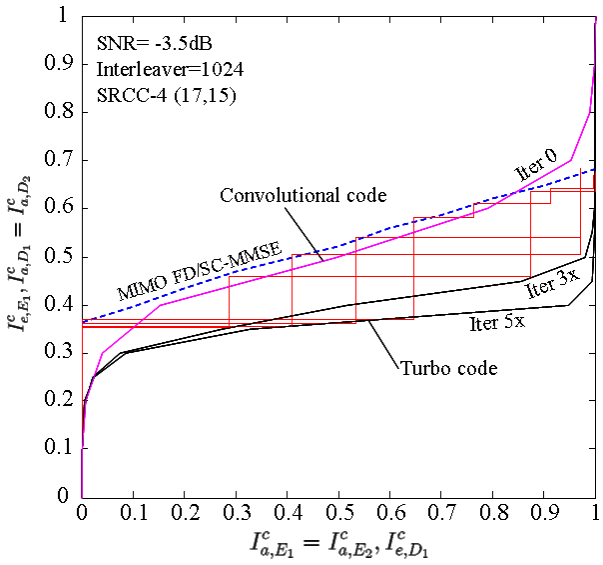

(a) Horizontal Iteration

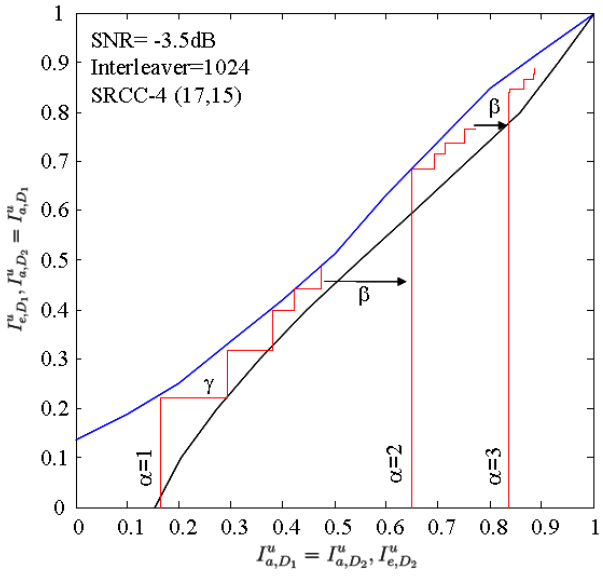

(b) Vertical Iteration

Fig. 5. Trajectory analysis at SNR = -3.5dB

V. Performances Evaluation

To evaluate the performances, computer simulations were conducted using the parameters as shown in Table I. Block length is 512 and added by cyclic prefix (CP) with length of 64. All interleavers are random with length of 1024 for Π_1 and Π_2, while the length of Π_0 for the uncoded bits is 512.

BER performance results is shown in Fig. 6 assuming that channel has 64-path Rayleigh fading channel with equal average path gains. The receiver has perfect knowledge about the channel. Perfect block synchronization is assumed. The SNR is defined as average SNR per antenna where the total average power of each receive antenna branch #n is controlled

TABLE I
SIMULATION PARAMETERS

	Parameter	Value(s)
Transmitter	Modulation	BPSK
	Block Length (K)	512
	Encoder	SRCC 4(17,15)
	Coding Rate	R=1/2
	Interleavers	Random, length=1024
	Guard Interval/CP	64
Channel	Rayleigh Fading	64-path Equal Average Path Gains
Receiver	Equalizer	MIMO-FD/SC-MMSE
	Decoder	Log-MAP BCJR
	Channel Estimation	Perfect
	Synchronization	Perfect

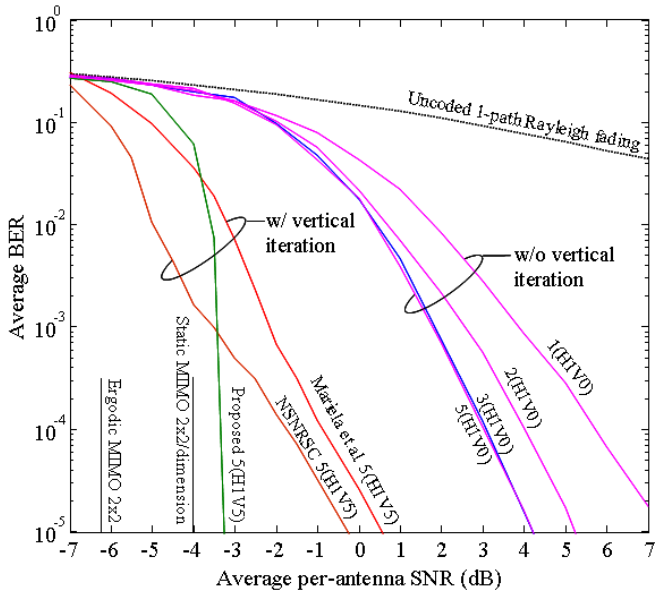

Fig. 6. BER Performances of the proposed STC (with SRCC), NSNRCC, Mariela et.al. [3], and a (Two-user) MIMO system

to satisfy

$$\left\langle \sum_{m=1}^{M} (\mathbf{h}_{n,m})(\mathbf{h}_{n,m})^H \right\rangle = 1. \quad (27)$$

First, the performances of the system without *VI* (equivalent to a multiuser MIMO system) are shown by the curves indexed by 1(H1V0), 1(H2V0), 1(H3V0) and 1(H5V0). However, because *VI* = 0, performance of 1(H2V0) is the same as 2(H1V0). Similarly, we have 1(H3V0) = 3(H1V0), 1(H5V0) = 5(H1V0), etc.

It is found that *HI* improves BER dominantly with its first iteration. The performance improvement by further iterations is not too significant especially after 3 iterations as shown by Fig. 6. Performance of 5(H1V0) is almost equal to 3(H1V0). The theoretical BER curve for uncoded BPSK is shown for a baseline comparison.

On the other hand, *VI* provides very significant improvement because we obtain the coding gain from SRCC into turbo processing. Therefore, when performing 5(H1V5) we have BER pinch-off at around average per-antenna SNR of -3.2dB by the pattern 5(H1V5), which is better compared to the case of when NSNRCC is applied, and system by Mariela et. al. in [3].

If we assume static non-fading channel, the capacity for 1/2 bits/channel with 2 transmit antennas is -4dB per dimension. It means that the simulation result is only within 1dB away from the static capacity limit/dimension, eventhough simulation assumes block fading and BER curves are in the sense of average.

VI. CONCLUSION

The spatial turbo coding has been presented using the MIMO FD/SC-MMSE turbo equalization that can achieve significant performance improvement over conventional spatial turbo code [3]. Recursive systematic code is better suited to this structure because it requires systematic bits in the vertical iterations. The proposed STC provide a BER pinch-off at average per-antenna SNR of about -3dB, which is within 1dB away from the static per dimension capacity limit of a 2×2 MIMO system.

REFERENCES

[1] Y. Liu and M. Fits, "Space-times turbo codes," in *37th Annual Allerton Conf. on Comm., Control and Comp.*, USA, 1999.

[2] M. Sellathurai, "On the performance of space-time turbo code," in *IEEE VTC 2005*, Sweden, May-June 2005.

[3] M. Sarestoniemi, T. Matsumoto, and M. Grossmann, "Coded space-time single carrier transmission with MMSE MIMO turbo equalization," in *IEEE Int. Symp. on Wireless Comm. Systems*, Spain, September 2006.

[4] K. Kansanen and T. Matsumoto, "An analitical method for MMSE MIMO turbo equalizer EXIT chart computation," *IEEE Trans. Wireless Comm.*, vol. 6, no. 1, pp. 59–63, Jan. 2007.

[5] Y. Liu, M. Fits, and O. Takeshita, "QPSK space-times turbo codes," in *IEEE Int. Conf. on Communications*, 2000, pp. 292–296.

[6] E. Huang, A. Gatherer, T. Muharemovic, and D. Hocevar, "Improving performance of a space-time turbo code in a Rayleigh faded channel," in *IEEE Vehicular Technology Conference (VTC)*, Oct. 2001.

[7] L. Bahl, J. Cocke, F. Jelinek, and J. Raviv, "Optimal decoding of linear codes for minimizing symbol error rate," *IEEE Trans. on Info. Theory*, vol. IT-20(2), pp. 284–287, March 1974.

[8] M. Tuchler, R. Koetter, and A. Singer, "Turbo equalization: Principles and new results," *IEEE Trans. on Comm.*, vol. 50, no. 5, pp. 754–767, May 2002.

[9] S. ten Brink, "Convergence behavior of iteratively decoded parallel concatenated codes," *IEEE Trans. Commun.*, vol. 49, pp. 1727–1737, Oct. 2001.

[10] M. Sarestoniemi, T. Matsumoto, K. Kansanen, and J. Iinatti, "Turbo diversity based on SC/MMSE equalization," *IEEE Transaction of Vehicular Technology*, vol. 54, no. 2, pp. 749–752, 2005.

[11] M. Sarestoniemi, T. Matsumoto, C. Schneider, and R. Thoma, "Channel measurement data based performance evaluation of coded space-time SC-MMSE MIMO turbo equalization," in *IEEE Int. Symp. on Wireless Comm. Systems*, Spain, Sept. 2006.

[12] I. Chatzigeorgiou, M. Rodrigues, I. Wassell, and R. Carasco, "Can punctured rate-1/2 turbo codes achieve a lower error floor than their rate-1/3 parent codes," in *IEEE Information Theory Workshop*, China, October 2006.